Precipitated Phases in a Weldment of P92 Steel

A.L. Marzocca[1], M. Zalazar[2], M.I. Luppo[1]

[1]National Atomic Energy Commission (CNEA), Buenos Aires, Argentina

[2]National University of Comahue, Neuquén, Argentina

E-mail contact of main author: marzocca@cnea.gov.ar

Abstract. The microstructural stability of ferritic-martensitic heat resistance steels is mainly controlled by the thermal stability of precipitates that are able to retard the growth rate of subgrains. The welded zones appear to be a weak region compared to the base material (BM) and creep rupture takes place in the intercritical or the fine-grained heat affected zones (ICHAZ and FGHAZ).

In the present work, precipitates of a single-pass weld performed by the flux-cored arc welding process in a P92 steel were identified by means of a transmission electron microscope on carbon replicas extracted from the BM and different regions generated during welding. In the BM, $M_{23}C_6$ carbides were the major precipitates, followed by VN, "wings" and NbCN. The dissolution of these precipitates took place during welding at different peak temperatures. $M_{23}C_6$ carbides were observed in the BM, ICHAZ and FGHAZ, VN were found in all zones, "wings" in the BM, ICHAZ and FGHAZ near the ICHAZ and NbCN were observed in all the HAZ.

It was observed that increasing the peak temperature (from the BM to the FZ) the size and quantity of precipitates decreased and they acquired a more spherical morphology. Moreover, the higher the peak temperature reached the greater the number of W-rich $M_{23}C_6$ carbides found.

Key Words: P92 steel, precipitates, FCAW process, microscopy.

1. Introduction

9-12%Cr ferritic/martensitic (F/M) steels are being considered for applications in Generation IV nuclear reactors as fuel cladding or core structures due to their superior resistance to irradiation embrittlement and radiation-induced swelling, higher thermal conductivity, lower thermal expansion, as well as good oxidation and corrosion resistance at elevated temperatures [1-3]. 9%Cr F/M steel grade P92 has being used in boiler components for ultra supercritical power plants operating up to 620°C because exhibits improved creep rupture properties compared to the first generation F/M steel developed for conventional power plants operating up to 565 °C [3] which makes it a promising candidate for cladding and duct applications in Sodium-Cooled Fast Reactor, one of the Generation IV nuclear energy systems [4].

F/M steels are supplied in a normalized and tempered condition. Their microstructure consists of lath martensite containing a high density of dislocations and precipitates: $M_{23}C_6$ and MX, where M denotes a metallic element and X is C and/or N atoms. The predominant $M_{23}C_6$ particles are mainly on lath boundaries and prior austenite grain boundaries (PAFBs) and their size is much larger in the vicinity of PAGBs than inside grains [5]. The size of the MX precipitates is much smaller than that of $M_{23}C_6$ carbides and they are distributed at laths, blocks, packet boundaries and PAGBs as well as in the matrix within laths. Zielinska-Lipiek [6] found in a P92 steel normalized at 970-1145 °C for 2 h and tempered at 715-835 °C for 2h $M_{23}C_6$ carbides and 3 types of MX precipitates: NbCN, plate-like VN and a complex MX

("wings") consisting of a spheroidal NbCN core which had nucleated a plate of VN "wings". The stability of $M_{23}C_6$ and MX is critical to the long term performance of these alloys [7].

The welding process strongly influences the microstructure and properties of the base material (BM). As a result of the severe thermal cycle caused by the welding process, the original microstructure is altered and a so-called heat affected zone (HAZ) is formed. The HAZ can be divided into a number of sub-zones: the coarse-grained zone (CGHAZ), the fine-grained zone (FGHAZ) and the intercritical zone (ICHAZ). No distinct borderline between the different regions is recognizable, it is more a continuous gradient from the fusion line between the deposited weld metal to the unaffected base material (BM). Each sub-zone is represented by its characteristic microstructure and properties [8].

Though significant improvements in the high temperature properties of the F/M steels have been achieved by alloy modification, creep properties of the weld joint have been found to be inferior to that of both the BM and the weld metal. This is due to the Type IV cracking, fracture in the HAZ of the weld joint during high temperature service or during creep test. ICHAZ (heated to a maximum temperature between A_{c1} and A_{c3}) and FGHAZ (heated just above A_{c3}) are known to be the locations where Type 4 cracking occurs [9].

Because precipitate phases may strikingly affect the creep resistance of F/M steels, the investigation of precipitate phases in welds, especially with regard to the fine grains zones is of great importance in understanding the effect of precipitates on the creep properties of the steels. Therefore, a detailed electron microscopy study was carried out in the base material (BM), fusion zone (FZ) and each sub-zone of the HAZ to identify the precipitates present in a single-pass weld performed by the flux-cored arc welding in a P92 steel.

2.   Experimental

A single-pass weld was performed in a pipe of an ASTM A335 P92 steel provided by Vallourec& Mannesmann, France, with a wall thickness of 9.53 mm and diameter of 73 mm. The material was received in the standard metallurgical condition, i.e., normalized at 1060 °C, 20 minutes and tempered at 780 °C, 60 minutes. The chemical composition is shown in Table I. The process employed was flux-cored arc welding (FCAW) under 80%Ar/20%CO_2 gas shielding. The filler material was a rutilic slag wire 9Cr0.5Mo1W – Supercore F92 (E9T1-G) whose chemical composition is shown in Table I. The preheat temperature was 260 °C and the welding parameters were: welding voltage 26 V, welding current 160A, welding speed 20 cm/min, weld heat input 1.26 kJ/mm.

TABLE I: CHEMICAL COMPOSITION OF P92 AND F92 IN WT. %.

Alloy	C	Cr	Mo	W	Si	V	Nb	N	Mn	Ni	Al	B
P92	0.13	8.72	0.38	1.63	0.24	0.2	0.06	0.05	0.46	0.17	0.01	0.002
F92	0.11	9	0.45	1.7	0.30	0.2	0.04	0.04	0.8	0.5	<0.01	0.003

The metallographic preparation was carried out by polishing up to diamond paste down to 1 µm and etching with the Villela´s reagent. An Olympus X51 optical microscope was used to identify each sub-zone of the HAZ. The distribution of the precipitates in the matrix was observed by means of a Zeiss Supra 40 scanning electron microscope with field emission gun (FEG-SEM). The identification of precipitates was carried out in a Phillips CM200 (TEM)

equipped with an EDAX-DX4 system for energy dispersive analysis of X-rays (EDS) on carbon replicas extracted from the BM, FZ and each sub-zone of the HAZ. In the present work the precipitates were identified by means of their selected area diffraction pattern (SADP) and/or their EDS spectrum. The criterion assumed to differentiate NbCN from VN was: VN when the corresponding EDS spectrum displayed a V- Kα line more intense than the Nb-Lα line and vice versa for the NbCN particles.

3. Results and discussion

SEM micrographs in Fig. 1 (a-e) show a general view of the zones recognized in a single-pass weld of a P92 steel.
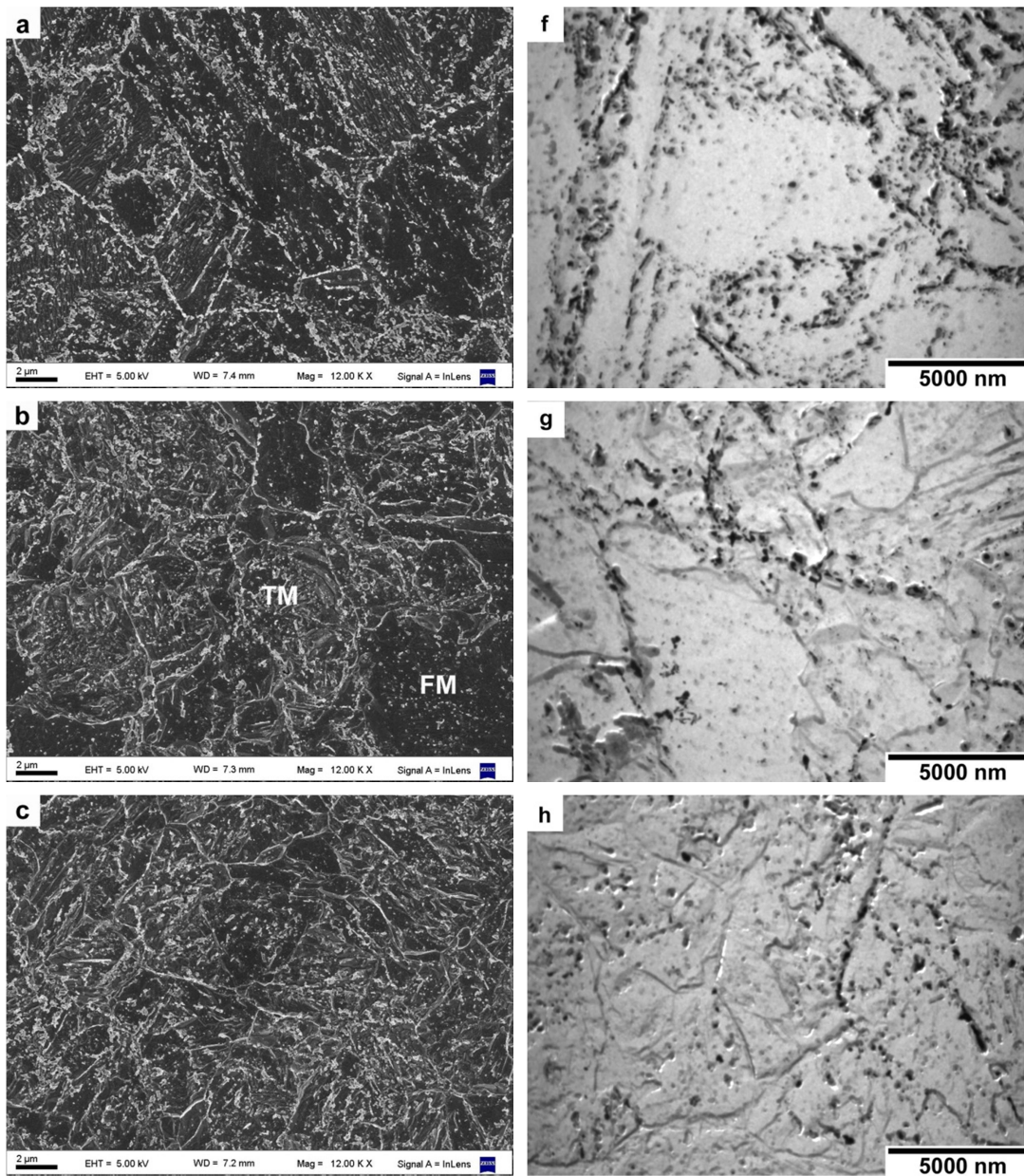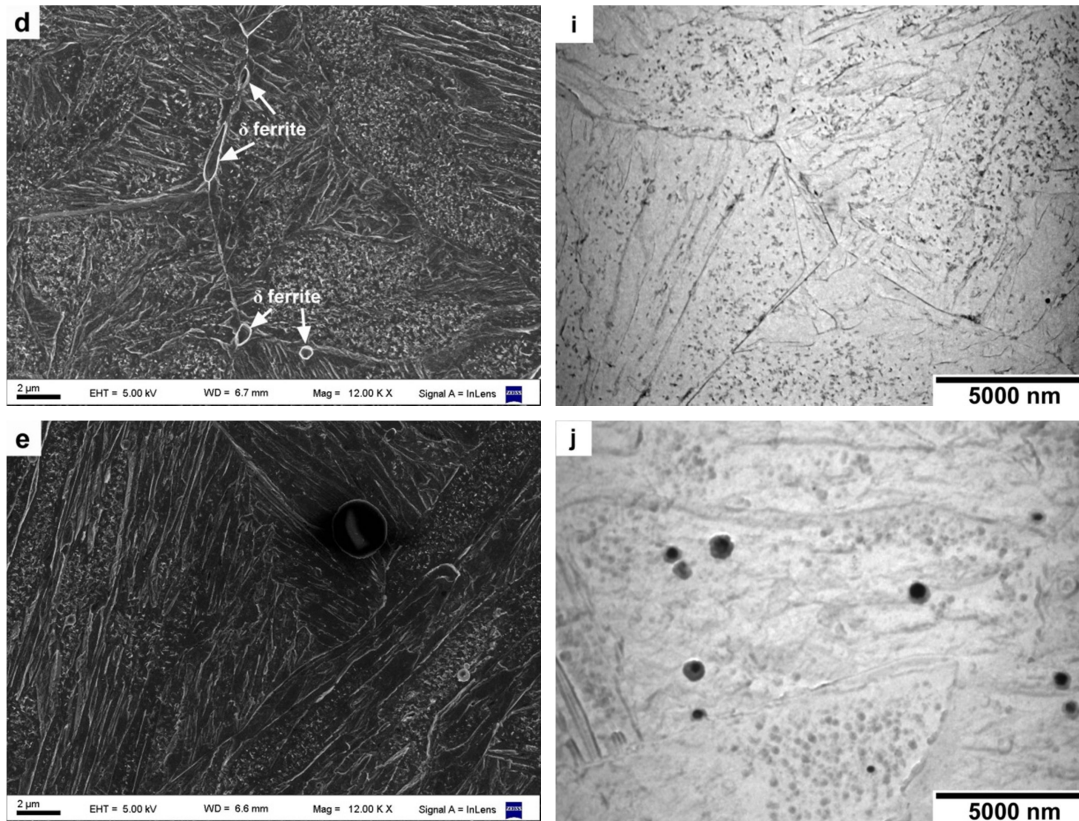
FIG. 1. SEM (left) and TEM (right) micrographs of the: BM (a and f), ICGHAZ (b and g), FGHAZ (c and h), CGHAZ (d and i) and FZ (e and j).

The BM in the as-welded sample is the zone that was not affected during welding, i.e., the material in the as-received condition. The microstructure consists of tempered lath martensite (Fig. 1.a) with precipitates on lath boundaries, prior austenite grain boundaries and inside grains.

In the ICHAZ a partial transformation of martensite into austenite result on heating during welding, then in this sub-zone coexist a new fresh martensite (FM) and the tempered original microstructure (TM) as it is shown in Fig. 1.b.

Peak temperatures reached in the FGHAZ may not be enough to dissolve precipitates completely, limiting the grain growth by pinning the austenite grain boundaries. On cooling, a fine grained FM microstructure is formed (see Fig. 1.c).

The CGHAZ is the sub-zone adjacent to the fusion line and it experiences temperatures well above the A_{c3} transformation temperature. Any precipitates that obstruct growth of austenite grains at lower temperatures dissolve, resulting in coarse grains of austenite (Fig. 1.d). In F/M steels δ-ferrite grains may nucleate at the highest peak temperatures (> 1250°C) causing overall grain size to decrease [8]. δ-ferrite grains were observed in some grain boundaries of the CGHAZ as it is indicated in Fig. 1.d.

The FZ (Fig. 1.e) represents the region that had liquefied during welding and shows columnar grains with a large amount of inclusions associated with the nature of the flux used during the FCAW welding.

It was observed that increasing the peak temperature (from the BM to the FZ) the size and quantity of precipitates decreased and they acquired a more spherical morphology as it is

shown in TEM micrographs of Fig. 1. f-j. Moreover, some grain boundaries without precipitates are observed in the ICHAZ (Fig. 1.g) and FGHAZ (Fig. 1.h).

In the following sections, the identification of precipitates in the as-received condition and in the different regions of the single-pass weld will be presented.

3.1. Base material (BM)

Precipitates en the BM are the present in the as-received condition and they are the second phases that will evolve during the thermal cycles experienced during welding. $M_{23}C_6$ carbide was the major observed precipitate. The next precipitated phases identified as for the estimated volume fraction were: VN, then "wings" and a few NbCN. Ternary composition diagrams of $M_{23}C_6$ and MX are shown in Fig. 2.a and 2.b, respectively. The composition of the "wings" was not considered in the ternary composition diagram of MX particles. The chemical composition of $M_{23}C_6$ and MX precipitates exhibited a broad scatter. In the BM zone the Cr-rich was the major $M_{23}C_6$ observed (indicated as $M_{23}C_6$ in figures).
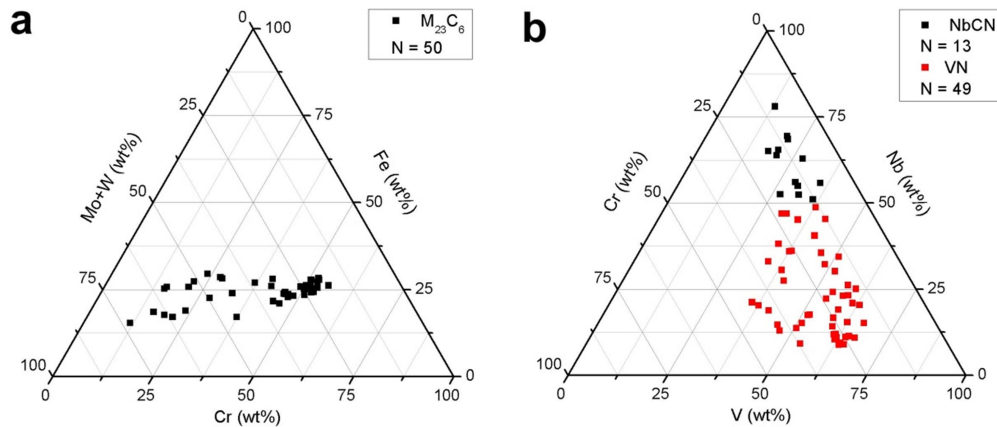

FIG. 2. Ternary composition diagrams of $M_{23}C_6$ (a) and MX (b) precipitates in the BM. N = number of particles.

$M_{23}C_6$ carbides in the BM exhibited several kinds of morphologies and selected area diffraction patterns (SADP) were indexed considering the spatial group 225-Fm-3 with a lattice parameter of 1.066 nm.
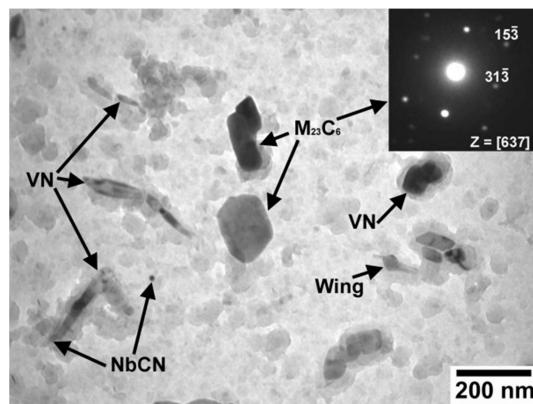

FIG. 3. TEM micrograph of the BM. The inset shows the SADP of the $M_{23}C_6$.

VN precipitates are isolated or forming clusters as it is shown in Fig. 3. Moreover, diffraction rings in accordance of the VN precipitates were observed everywhere of the BM carbon replicas (Fig. 4). The SADP matches well with a particle belonging to a spatial group 225-Fm-3 and a lattice parameter of 0.41295 nm.

"Wings" and NbCN are showed in Figure 3. SADP of wings shows a pattern corresponding to VN wings and a core than matched well with the SADP from NbCN (spatial group: 225-Fm-3; a = 0.44082 nm).
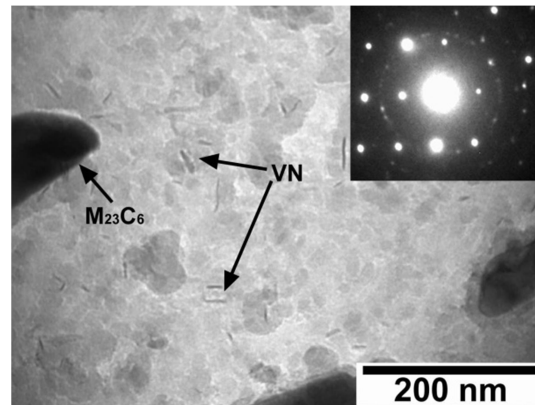

FIG. 4. TEM micrograph of the BM. The inset shows a ring pattern that corresponds to fine VN precipitates and a spot pattern that correspond to the indicated $M_{23}C_6$ carbide.

Minority particles as primary NbCN are very difficult to recognize because their morphology and size are similar to $M_{23}C_6$ carbides. Fig. 5.a shows a primary NbCN with a chemical composition of 78.4Nb-13.8V-11.4Cr (without Ti) or 70.2Nb-14.6V-8.3Ti-6.9Cr (with Ti) and a ring pattern that corresponds to VN particles. A dark field obtained using a part of the first ring shows a very fine dispersion of VN precipitates in the BM matrix (Fig. 5.b).
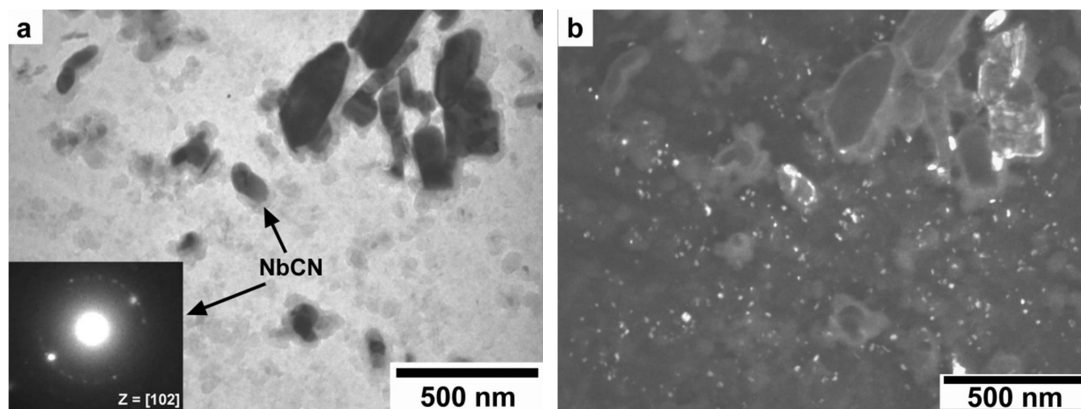

FIG. 5. TEM micrograph of the BM showing: (a) spots in the SADP correspond to the primary NbCN precipitate and a ring pattern corresponds to VN. (b) Dark field showing the fine VN precipitates.

3.2. Intercritical heat affected zone (ICHAZ)

Precipitates in the ICHAZ were the same that were found in the BM, but in some places (indicated by arrows in Fig. 6.a) "wings" were the major observed precipitated, followed by VN, then NbCN and a few $M_{23}C_6$ (Fig. 6.b).
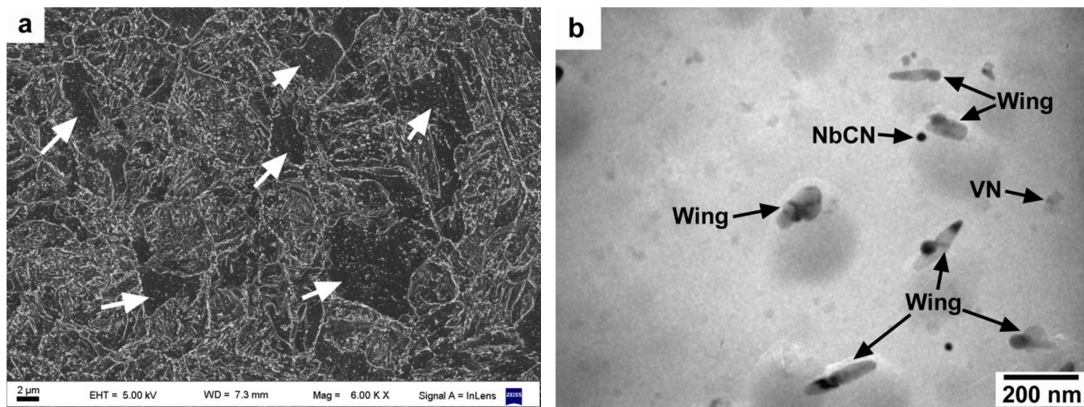
FIG. 6. a) SEM micrograph of the ICHAZ. b) TEM micrograph of one of the zones indicated by arrows in a) where "wings" were the major observed precipitates (zones indicated by arrows in a).

3.3. Fine-grained heat affected zone (FGHAZ)

Fig. 7 shows the precipitates identified in the FGHAZ as the peak temperatures rises.
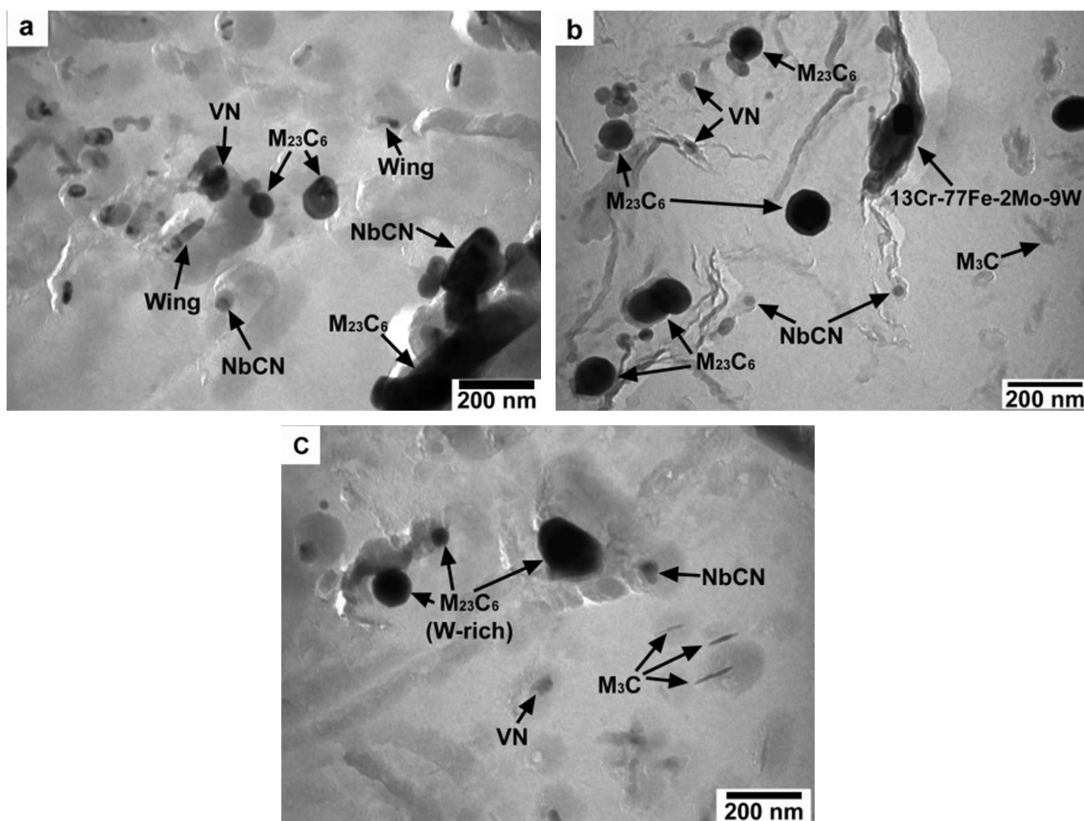

FIG. 7. TEM micrographs of the FGHAZ: a) near ICHAZ, b) intermediate ICHAZ and b) near CGHAZ.

In the FGHAZ near the ICHAZ (Fig. 7.a) the identified precipitates were the same that were found in the BM. In the intermediate zone of the FGHAZ begins to decrease more abruptly the quantity of precipitates, but the Cr-rich $M_{23}C_6$ carbide continue being the major observed precipitate (Fig. 7.b). M_3Fe (21Cr-79Fe) precipitates of elongated shape were observed in this zone and their presence is attributed to the autotempering of martensite. No more "wings"

were observed from the intermediate zone of the FGHAZ. Near the CGHAZ (Fig. 7.c) the quantity of W-rich $M_{23}C_6$ was higher than the quantity of Cr-rich $M_{23}C_6$. Moreover, near the CGHAZ the quantity of precipitates is too low that it was easier to recognize the primary NbCN precipitates. Precipitates with a high Fe content (13Cr-77Fe-2Mo-9W) were observed in the intermediate FGHAZ and near the CGHAZ. These particles have not been identified yet.

Ternary composition diagrams of $M_{23}C_6$ and MX precipitates are shown in Fig. 8.a and 8.b, respectively. A change in the distribution of solutes in M of $M_{23}C_6$ precipitates was observed between the BM (Fig. 2) and the FGHAZ: the higher the peak temperature reached the greater the number of W-rich $M_{23}C_6$ carbides found. Although the amount of MX precipitates identified in the FGHAZ (Fig. 8.b) was not as high as those identified in the BM (Fig. 2.b), it would seem that the NbCN precipitates increased their Nb content at expense of their V content.
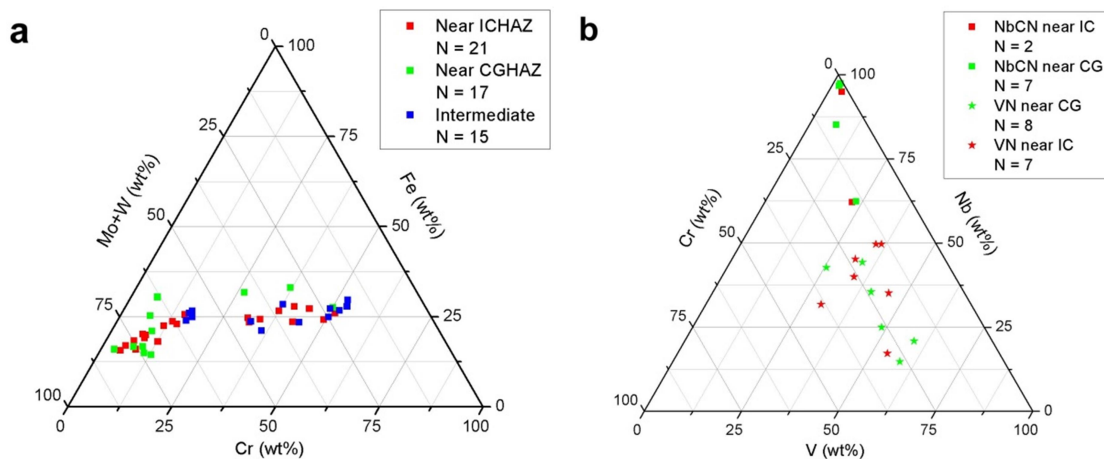

FIG. 8. Ternary composition diagrams of $M_{23}C_6$ (a) and MX (b) precipitates in the FGHAZ. N = number of particles.

3.4. Coarse-grained heat affected zone (CGHAZ)

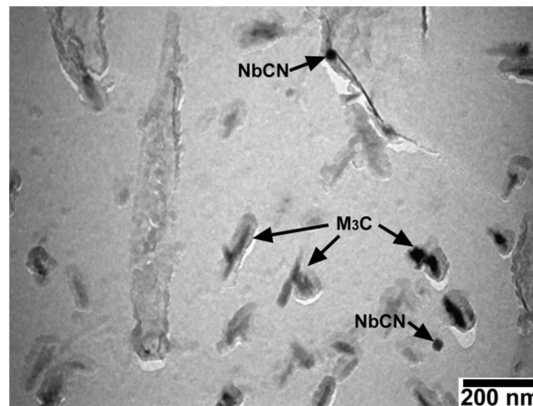The CGHAZ showed M_3C and primary NbCN particles (see Fig. 9).

FIG. 9. TEM micrograph of the CGHAZ.

A very few VN were observed in the CGHAZ.

3.5.δ-ferrite phase in the fusion line

δ-ferrite phase was observed in the limit between the CGHAZ and the FZ as it is shown in Fig. 10.a. Two kinds of precipitates were found inside δ-ferrite phase: M_3C and Ti-MX (Fig. 10.b). The SADP of Ti-MX particles matches well with a spatial group and a lattice parameter corresponding to NbCN, but its chemical composition shows an increase in Ti content (43.2Nb-16.2V-29Ti-11.3Cr).
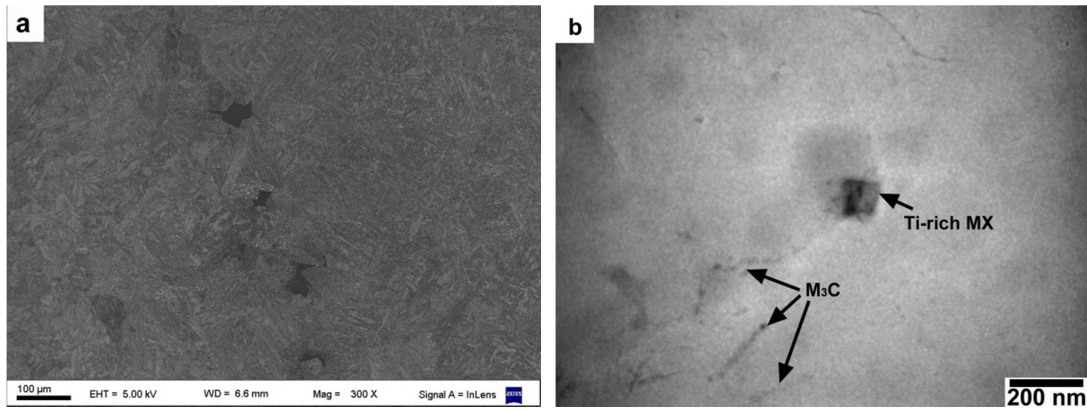

FIG. 10. a) SEM micrograph of the fusion line. b) Precipitates in δ-ferrite (TEM micrograph).

3.6.δ-Fusion zone (FZ)

The FZ has a large amount of inclusions. M_3C, Ti-rich MX and a few VN particles were recognized in this zone (Fig. 11).
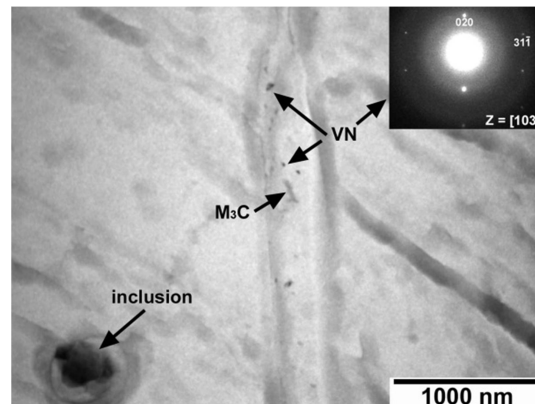

FIG. 11. TEM micrographs of precipitates in the FZ.

4. Conclusions

In the present study precipitates of a single-pass weld performed by the FCAW process in a P92 steel were identified by means of a transmission electron microscope on carbon replicas extracted from the BM and different regions generated during welding. In the BM the $M_{23}C_6$ carbides were the major precipitates, followed by the VN, "wings" and NbCN. The dissolution of these precipitates took place during welding at different peak temperatures and due to the high rates experienced during welding, the dissolution was deferred to temperatures

higher than those predicted by equilibrium conditions (~900 °C for $M_{23}C_6$ and ~1160 °C for MX). $M_{23}C_6$ carbides were observed in the BM, ICHAZ and FGHAZ; VN and NbCN precipitates were found in all zones and "wings" in the BM, ICHAZ and FGHAZ near ICHAZ. Moreover, the higher the peak temperature reached the greater the number of W-rich $M_{23}C_6$ carbides found.

By means of the observation of carbon replica extracted from each zone of a single pass weld it is possible to conclude that increasing the peak temperature (from the BM to the FZ) the size and quantity of precipitates decreased and they acquired a more spherical morphology. The cause of these variations is related to the differences in the thermal cycle to which each region was subjected. Incomplete transformation of austenite and additional tempering of the original tempered martensite structure of the BM occurs during heating in the ICHAZ. The FGHAZ is heated into the lower part of the γ-phase field where some of the original precipitates are not dissolved and inhibit grain growth. In the CGHAZ the original precipitates are dissolved, resulting in a coarse prior austenite grain.

This detailed information about the precipitates found in each region of the real HAZ could help to verify the correct behavior of a code that simulates a weld.

5. Acknowledgements

6. References

[1]   ABE, F., et al., "Development of reduced-activation martensitic 9Cr steels for fusion reactor", J. Nucl. Sc. Tech. **31** (1994) 279.

[2]   KLUEH, R.L., et al., "High chromium ferritic and martensitic steels for nuclear applications, American Society for Testing and Materials, West Conshohocken, Pennsylvania, 2001, pp. 5-38.

[3]   KLUEH, R.L., NELSON, A.T., "Ferritic/martensitic steels for next-generation reactors", J. Nucl. Mat. **371** (2007) 37.

[4]   TOPBASI, C., et al., "In Situ Study of Heave Ion Induced Radiation Damage in NF616 (P92) Alloy", J. Nucl. Mat. **425** (2012) 48.

[5]   ABE, F., "Precipitate design for creep strengthening of 9%Cr tempered martensitic steel for ultra-supercritical power plants", Sci. Technol. Adv. Mater. **9** (2008) 013002.

[6]   ZIELINSKA-LIPIEK, A., et al., "The influence of heat treatments on the microstructure of 9% Cr steels containing W", J. Mater. Process. Technol. **64** (1997) 397.

[7]   FRANCIS, J.A., et al., "Type IV cracking in ferritic power plant steels", Mat. Sc. Tech. **22** (2006) 1387.

[8]   CERJAK, H., et al., "Creep strength of welded joints of ferritic steels", Creep Resistant Steels, Cambridge, England (2008) 472-503.

[9]   ALBERT, S.K., et al., "Microstructural investigations on Type IV cracking in a high Cr steel", ISIJ Int. **42** (2002) 1467.